Cadmium(II) and Lead(II) Complexes with Novel Macrocyclic Receptors Derived from 1,10-Diaza-15-crown-5

David Esteban,[a] Daniel Bañobre,[a] Andrés de Blas,*[a] Teresa Rodríguez-Blas,*[a] Rufina Bastida,[b] Alejandro Macías,[b] Adolfo Rodríguez,[b] David E. Fenton,[c] Harry Adams,[c] and Jose Mahía[d]

Keywords: Cadmium / Crown compounds / Cryptands / Lead / Macrocyclic ligands

Two novel macrocycles, *N*,*N*′-bis(2-aminobenzyl)-1,10-diaza-15-crown-5 (L^1) and a non-symmetric cryptand incorporating a pyridinyl Schiff-base spacer (L^3), both derived from 1,10-diaza-15-crown-5, have been shown to act as receptors for lead(II) and cadmium(II) guests. The X-ray crystal structures reveal an *anti* conformation for the free ligand L^1, but a *syn* arrangement in the lead(II) complex, $[PbL^1](ClO_4)_2$. The corresponding cryptates of L^3 can be prepared by simple transmetallation reactions starting from the barium cryptate, showing the preference of L^3 for the heavy metal ions. The lead(II) ion, unlike cadmium(II), has been shown to be capable of acting as a template agent in the synthesis of L^3. The X-ray crystal structures of the metal cryptates allow an insight into the influence of the nature of the metal ion guest on the conformation of the macrobicyclic receptor L^3; the most significant changes are a different folding of the crown and variations in the distance between the two pivotal nitrogen atoms and the imine nitrogen atoms. The cryptand can thus expand or contract its cavity in order to accommodate the different metal ions.

Introduction

The coordination chemistry of macrocyclic ligands is currently a fascinating area of intense study for inorganic chemists. One aspect of the interest that macrocyclic ligands have promoted stems from the fact that depending on features such as the nature, number, and arrangement of the ligand donors, ligand conjugation, substitution, and flexibility, the nature of the ligand backbone, macrocyclic hole size, and the number and sizes of the chelate rings, it is possible to tailor-make different types of macrocyclic molecules for specific uses. Thus, such systems can be used as models for biological systems, to study magnetic exchange phenomena, as synthetic ionophores, to study guest−host interactions, or as therapeutic reagents for the treatment of metal intoxication. In particular, macrocycles have been widely studied as complexing agents that may be used for the selective extraction of heavy and precious metals,[1−3] an area of great interest in environmental chemistry. Furthermore, the development of new technologies in this field depends on the design of new receptors capable of binding metal ions selectively or specifically.

The direct synthesis of a free macrocycle from its organic precursors often results in a low yield of the desired cyclic product, with side reactions such as polymerization predominating. Consequently, synthetic strategies such as the use of high dilution conditions, the incorporation of a rigid group in the open-chain precursors, and the use of template agents have been developed. In a previous paper,[4] we described a synthetic route for preparing a novel family of Schiff-base cryptands derived from bibracchial lariat ethers incorporating pendant aniline moieties and various dialdehyde functions (Scheme 1; L^3, L^4, L^5, L^6). Structurally, these systems belong to the group defined as lateral macrobicycles.[5] We found that they can not be prepared by direct reaction between the organic precursors, but that barium(II) ion can act as a template, thereby allowing access to the required macrobicycles in high yields.

Here, we describe lead(II) and cadmium(II) complexes with the receptors L^1 and L^3 (Scheme 1), macrocycles belonging to two different structural classes, namely bibracchial lariat ethers and cryptands, respectively. The lariat ethers constitute a sub-class of macrocyclic polyethers and are characterized by the presence of one (monobracchial) or more (polybracchial) side-arms attached to pivotal atoms of the parent macrocyclic ring. The incorporation of additional donor atoms in the side arms can be used to enhance the coordination potential of these polybracchial ligands. These compounds may be regarded as having structural characteristics intermediate between those of flexible mac-

[a] Departamento Química Fundamental e Industrial, Universidade da Coruña, Campus da Zapateira s/n, E-15071 La Coruña, Spain
Fax: (internat.) +34−981/167000
E-mail: mayter@udc.es
[b] Departamento Química Inorgánica, Universidad de Santiago, Avda. de las Ciencias s/n, E-15706 Santiago de Compostela, Spain
[c] Chemistry Department, The University, Sheffield S3 7HF, U.K.
[d] Servicios Xerais de Apoio á Investigación, Universidade da Coruña, Campus da Zapateira s/n, E-15071 La Coruña, Spain

  1434−1948/00/0707−1445 $ 17.50+.50/0

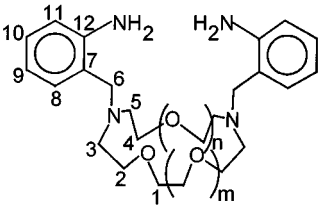

L^1: n = m = 1
L^2: n = 2, m = 1

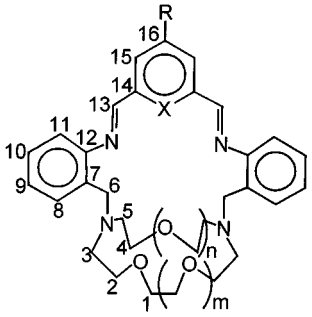

	n	m	R	X
L^3	1	1	H	N
L^4	1	1	CH_3	C-OH
L^5	2	1	H	N
L^6	2	1	CH_3	C-OH

Scheme 1

rocyclic polyethers and relatively rigid macrobicyclic cages or cryptands.

Two issues are addressed in the present paper. Firstly, we have studied different synthetic routes and strategies for preparing lead(II) and cadmium(II) complexes with the macrobicycle L^3. Secondly, we have carried out structural studies to assess the different complexation capabilities of the two classes of macrocycles towards the heavy metal ions lead(II) and cadmium(II) as well as the influence of the nature of the metal ion guest on the conformation of the macrobicycle receptor L^3.

Results

Synthesis and Characterization of the Bibracchial Lariat Ether L^1 and its Cadmium(II) and Lead(II) Complexes

Our synthetic route to the novel bibracchial lariat ether L^1 involves two key steps, specifically *N*-binding of 2-nitrobenzyl chloride to the diaza-crown and subsequent reduction of the NO_2 groups of the resulting *N*,*N*′-bis(2-nitrobenzyl)-diaza-crown to $-NH_2$ groups with hydrazine hydrate in the presence of Pd/C as a catalyst. The synthesis can be carried out in a one-pot procedure by reducing the intermediate *N*,*N*′-bis(2-nitrobenzyl)-diaza-crown prepared in situ. In this way, better yields are obtained. Single crystals of L^1 suitable for X-ray diffraction analysis were grown by slow evaporation of the solvents from an absolute ethanol/diethyl ether (1:1) solution. As expected, the IR spectrum (KBr discs) features two bands due to a $\nu_{as}(NH_2)$ mode at 3430 and 3390 cm^{-1}, and two further bands corresponding to a $\nu_s(NH_2)$ mode at 3293 and 3275 cm^{-1}.

Reactions of the perchlorate salts $M(ClO_4)_2 \cdot n\,H_2O$ (M = Pb, Cd) with the bibracchial lariat ether L^1 yielded the complexes $[PbL^1](ClO_4)_2$ (**1**) and $[CdL^1](ClO_4)_2$ (**2**). Both were isolated as white solids. Colourless crystals of **1** suitable for single-crystal X-ray diffraction analysis were grown by allowing diethyl ether to diffuse into an acetonitrile solution of the complex. In the IR spectra (KBr discs), the amine groups give rise to $\nu_{as}(NH_2)$ and $\nu_s(NH_2)$ stretching bands at 3334 and 3277 cm^{-1} for **1** and at 3320 and 3281 cm^{-1} for **2**. Bands corresponding to the $\nu_{as}(ClO)$ stretching and $\delta_{as}(O-Cl-O)$ bending modes of the perchlorate groups appear without splitting at ca. 1100 and 625 cm^{-1}, respectively, as befits an uncoordinated anion.

The molar conductivities of the complexes at 20 °C in a ca. 10^{-3} M acetonitrile solution were measured as Λ_M = 285 $cm^2 \cdot \Omega^{-1} \cdot mol^{-1}$ for **1** and 289 $cm^2 \cdot \Omega^{-1} \cdot mol^{-1}$ for **2**. These data reveal that both complexes behave as 2:1 electrolytes in this solvent, and hence are completely dissociated.[6]

The ^1H- (Table 1) and ^{13}C-NMR spectra of the complexes were recorded in CD_3CN solution. The ^1H-NMR spectra of the complexes are clearly more complicated than that of the free lariat ether L^1. This is particularly apparent in the region $\delta = 0-4$, where signals due to the protons of the ethylenic and methylenic chains are observed. On coordination, the ligand becomes more rigid, restricting any exchange, and so the protons become non-equivalent and give rise to more signals. While the signals due to the aromatic protons are shifted downfield by ca. 0.5 ppm in the complexes, the signal due to the amine protons is shifted upfield by 0.79 ppm in **1** and by 0.04 ppm in **2** as compared to its position in the spectrum of the free ligand, thus confirming the coordination of the amine groups to the metal.

The UV/vis spectrum of the free ligand L^1, recorded in acetonitrile solution, features three absorption bands at λ_{max} = 213, 237, and 284 nm, corresponding to E_1, E_2, and B charge-transfer bands of the aromatic rings, respectively. The spectra of the complexes also feature the three expected bands, at λ_{max} = 209, 228, and 272 nm for **1**, and 213, 226, and 274 nm for **2**, shifted to lower wavelengths due to the coordination of the amine groups.

X-ray Crystal Structures of L^1 and 1

The crystal structure of the free receptor L^1 is shown in Figure 1; selected bond lengths and angles are given in Table 2. The arms of the lariat ether are arranged on opposite sides of the crown moiety resulting in an *anti* conformation. The crystal packing is determined by intermolecular hydrogen-bonds, which involve one proton of the amine group and an oxygen atom of the neighbouring molecule. Weak intramolecular hydrogen-bonds exist between the amine groups and the pivotal nitrogen atoms, with N(pivotal)···HN(amine) bond lengths of 2.362 and 2.339 Å, N(amine)···N(pivotal) bond lengths of 2.959 and 2.894 Å, and N(amine)−H−N(pivotal) angles of 123.8° and 119.8°.

Table 1. ^{1}H-NMR data for L^1 and its complexes

[a]	NH_2	H-11	H-9	H-10	H-8	H-5	H-3	H-6	H-2	H-1	H-4
L^{1}[b]	4.99(s), 4H	6.62(d), 2H	6.57 (t), 2H	7.04 (t), 2H	6.96 (d), 2H	←2.62 (m), 8H→		←3.51 (m), 16H→			
1 [c]	4.20(s), 4H	7.12 (d), 2H	7.03 (t), 2H	7.45 (t), 2H	7.29 (d), 2H	←2.90 (m), 8H→		←3.18 (m), 16H→			
2 [d]	4.95(s), 4H	←7.16 (m), 4H→		←7.39 (t), 4H→		←2.80 -3.83 (m), 24H→					

[a] See Scheme 1 for labelling. – [b] Conditions: T = 293 K, CD_3CN, 500 MHz. Assignment supported by 2D H,H COSY, HMQC, and HMBC experiments. $J_{2,3}$ = 7.08 Hz, $J_{4,3} = J_{4,5}$ = 7.48 Hz, $J_{3,2} = J_{3,4}$ = 7.48 Hz, $J_{5,4}$ = 7.35 Hz. Chemical shifts (without assignment) of the different multiplets for crown protons are given only. – [c] Conditions: T = 293 K, CD_3CN, 200 MHz. $J_{2,3}$ = 7.33 Hz, $J_{4,3} = J_{4,5}$ = 7.32 Hz, $J_{3,2} = J_{3,4}$ = 7.81 Hz, $J_{5,4}$ = 7.81 Hz. Chemical shifts (without assignment) of the different multiplets for crown protons are given only. – [d] Conditions: T = 293 K, CD_3CN, 200 MHz. Chemical shifts (without assignment) of the different multiplets for crown and/or aromatic protons are given only.

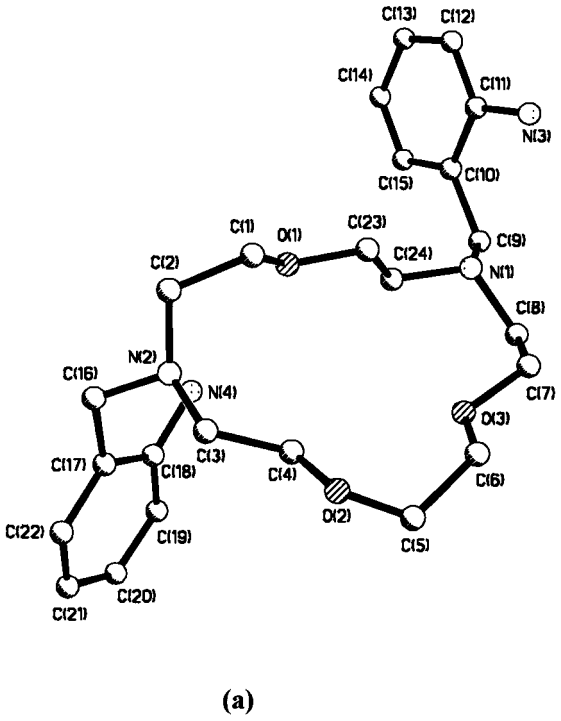

(a)

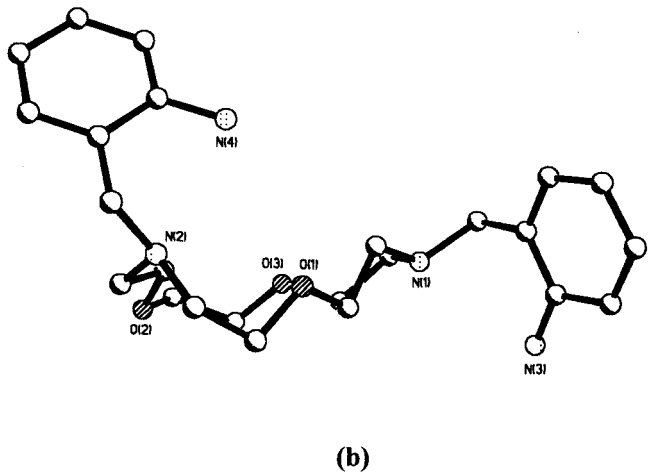

(b)

Figure 1. X-ray crystal structure of the bibracchial lariat ether L^1 showing the atomic numbering scheme; hydrogen atoms are omitted for the sake of clarity: (a) frontal view, (b) side view

Table 2. Selected distances [Å] and angles [deg] in the bibracchial lariat ether L^1 and complex **1**

L^1			
N(1)–C(24)	1.472(3)	N(2)–C(16)	1.465(3)
N(1)–C(9)	1.476(4)	N(2)–C(3)	1.466(4)
N(1)–C(8)	1.476(4)	N(2)–C(2)	1.461(3)
N(3)–C(11)	1.389(4)	N(4)–C(18)	1.383(4)
C(24)–N(1)–C(8)	113.6(2)	C(16)–N(2)–C(3)	114.3(2)
C(8)–N(1)–C(9)	109.0(2)	N(3)–C(11)–C(10)	119.5(3)
C(24)–N(1)–C(9)	110.9(2)	N(1)–C(9)–C(10)	114.5(2)
C(2)–N(2)–C(3)	114.8(2)	N(4)–C(18)–C(17)	119.8(2)
C(2)–N(2)–C(16)	113.0(2)	N(2)–C(16)–C(17)	112.1(2)
C(23)–O(1)–C(1)	114.6(2)	C(4)–O(2)–C(5)	114.2(3)
C(7)–O(3)–C(6)	111.5(2)		
1			
Pb(1)–O(3)	2.568(5)	Pb(1)–O(2)	2.702(6)
Pb(1)–N(4)	2.652(7)	Pb(1)–O(1)	2.732(6)
Pb(1)–N(2)	2.688(7)	Pb(1)–N(1)	2.757(6)
O(3)–Pb(1)–N(4)	81.6(2)	N(2)–Pb(1)–O(2)	62.9(2)
O(3)–Pb(1)–N(2)	64.2(2)	O(3)–Pb(1)–O(1)	81.3(2)
N(4)–Pb(1)–N(2)	75.1(2)	N(4)–Pb(1)–O(1)	160.0(2)
O(3)–Pb(1)–O(2)	97.2(2)	N(2)–Pb(1)–O(1)	106.3(2)
N(4)–Pb(1)–O(2)	133.1(2)	O(2)–Pb(1)–O(1)	59.7(2)
O(3)–Pb(1)–N(1)	63.2(2)	N(4)–Pb(1)–N(1)	98.2(2)
N(2)–Pb(1)–N(1)	127.4(2)	O(2)–Pb(1)–N(1)	123.3(2)
O(1)–Pb(1)–N(1)	64.7(2)		

Figure 2 illustrates the crystal structure of the complex cation $[PbL^1]^{2+}$ of **1**, while Table 2 provides a listing of selected bond lengths and angles. Only six of the seven available donor atoms of L^1 are coordinated to the lead(II) ion with one of the aniline pendant arms uncoordinated. The metal ion lies 1.71 Å above the plane defined by the three ether oxygen atoms and is asymmetrically disposed with respect to the crown ether moiety being closer to O(3) [Pb–O(3) 2.568(5) Å] than to the other oxygen atoms [Pb–O(2) 2.702(6) Å, Pb–O(1) 2.732(6) Å]. All of these distances fall within the ranges reported for the $Pb-O_{ether}$ bonds in lead(II)–crown ether complexes.[7] The lead(II) atom lies closer to the pivotal nitrogen atom bearing the coordinating pendant arm [Pb–N(2) 2.688(7) Å] than to the pivotal nitrogen atom bearing the non-coordinating pendant arm [Pb–N(1) 2.757(6) Å]. The lead atom and the donor atoms O(3), N(1), and N(2) are essentially coplanar, with a deviation from planarity of just 0.0118 Å. This may be viewed as an equatorial plane with oxygen atoms O(2) and O(1) located 2.2017 Å and 2.4650 Å above it and the

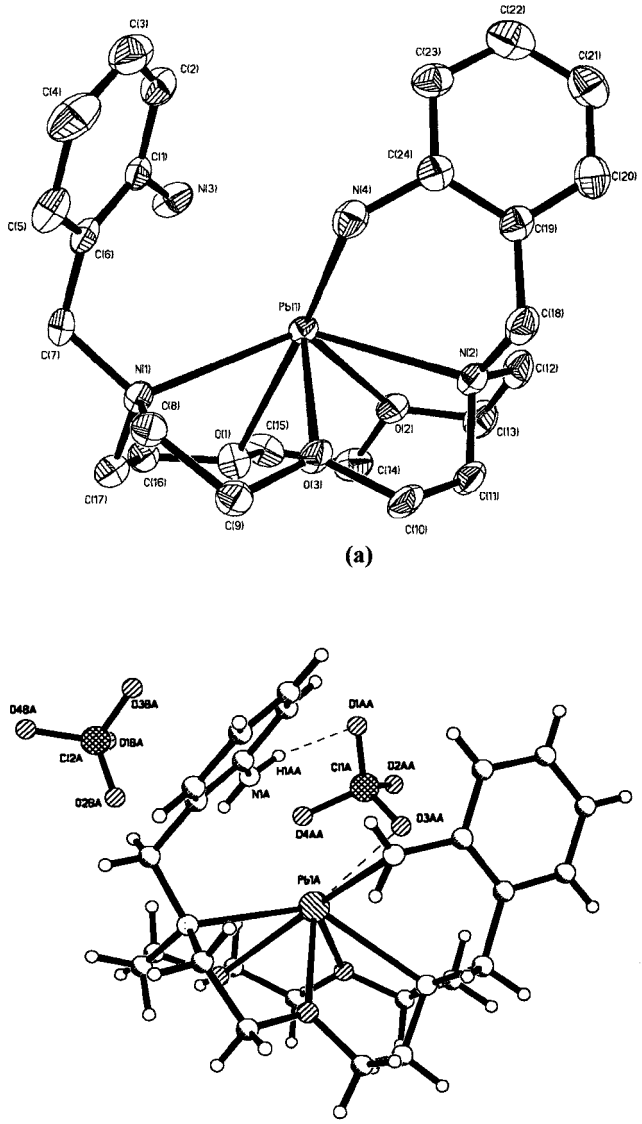

Figure 2. (a) X-ray crystal structure of the cationic complex $[PbL^1]^{2+}$ showing the atomic numbering scheme; hydrogen atoms are omitted for the sake of clarity; the ORTEP plot is drawn at a 30% probability level; (b) X-ray crystal structure of **1**

nitrogen atom N(4) lying 2.568 Å beneath it. The coordination polyhedron at the metal may be described as a dodecahedron with two unoccupied sites (Figure 3). The presence of these unoccupied sites leads to an empty zone in the coordination sphere at the metal, as indicated in Figure 3.

From a recent extensive survey of lone-pair functionality in lead(II) complexes, it has emerged that two distinct structural groups, with geometries that are holo-directed and hemi-directed, are possible. In the former group, the metal−ligand bonds can be directed to any point on the surface of an encompassing globe, whereas in the latter group there is a distinct void, or empty zone, in the global array of ligands.[8] The presence of such a void in the angular distribution of the coordination sphere about lead(II) is

Table 3. Selected distances [Å] and angles [deg] in complexes **3** and **4**

3			
Pb(1)−O(3)	2.670(6)	Pb(1)−O(1)	2.718(6)
Pb(1)−N(5)	2.703(6)	Pb(1)−O(2)	2.719(6)
Pb(1)−O(10)	2.714(8)	Pb(1)−N(4)	2.740(6)
Pb(1)−N(2)	2.744(6)		
O(3)−Pb(1)−N(5)	140.5(2)	N(5)−Pb(1)−O(2)	122.1(2)
O(3)−Pb(1)−O(10)	74.4(3)	O(10)−Pb(1)−O(2)	138.6(3)
N(5)−Pb(1)−O(10)	73.3(2)	O(10)−Pb(1)−O(1)	155.6(2)
O(3)−Pb(1)−O(1)	124.6(2)	O(3)−Pb(1)−O(2)	97.2(2)
N(5)−Pb(1)−O(1)	82.9(2)	O(1)−Pb(1)−O(2)	60.1(2)
O(3)−Pb(1)−N(4)	137.6(2)	N(5)−Pb(1)−N(4)	61.0(2)
O(10)−Pb(1)−N(4)	85.8(3)	O(1)−Pb(1)−N(4)	87.1(2)
O(1)−Pb(1)−N(4)	87.1(2)	O(2)−Pb(1)−N(4)	73.4(2)
O(2)−Pb(1)−N(4)	73.4(2)	O(3)−Pb(1)−N(2)	65.1(2)
N(5)−Pb(1)−N(2)	128.6(2)	O(10)−Pb(1)−N(2)	79.2(2)
O(1)−Pb(1)−N(2)	121.1(2)	O(2)−Pb(1)−N(2)	61.0(2)
N(4)−Pb(1)−N(2)	74.6(2)		
4			
Cd(1)−N(1)	2.349(10)	Cd(1)−N(4)	2.419(11)
Cd(1)−N(5)	2.366(9)	Cd(1)−O(3)	2.459(8)
Cd(1)−O(1)	2.374(11)	Cd(1)−O(2)	2.493(9)
Cd(1)−N(3)	2.566(10)		
N(1)−Cd(1)−N(5)	129.7(3)	N(5)−Cd(1)−O(2)	77.7(3)
N(1)−Cd(1)−O(1)	72.8(3)	O(1)−Cd(1)−O(2)	65.5(4)
N(5)−Cd(1)−O(1)	126.9(4)	N(4)−Cd(1)−O(2)	102.3(4)
N(1)−Cd(1)−N(4)	116.4(3)	O(3)−Cd(1)−O(2)	108.8(3)
N(5)−Cd(1)−N(4)	68.4(4)	N(1)−Cd(1)−N(3)	78.2(3)
O(1)−Cd(1)−N(4)	153.3(3)	N(5)−Cd(1)−N(3)	64.4(3)
N(1)−Cd(1)−O(3)	68.1(3)	O(1)−Cd(1)−N(3)	79.3(4)
N(5)−Cd(1)−O(3)	145.4(3)	N(4)−Cd(1)−N(3)	126.2(3)
O(1)−Cd(1)−O(3)	84.5(3)	O(3)−Cd(1)−N(3)	145.6(3)
N(4)−Cd(1)−O(3)	77.0(3)	O(2)−Cd(1)−N(3)	91.8(3)
N(1)−Cd(1)−O(2)	138.3(4)		

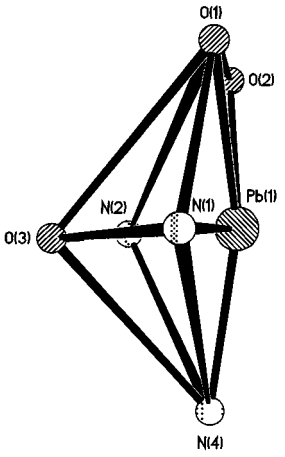

Figure 3. Coordination polyhedron of the cationic complex $[PbL^1]^{2+}$

usually taken as an indication of the presence of a stereochemically active lone pair of electrons on the lead atom.[9,10] It has also been suggested that there will be a concomitant shortening of the Pb−X bond on the side of the lead(II) away from the site of the stereochemically active lone pair.[9,11] In these hemi-directed compounds, the differences between Pb^{II}−X and Pb^{II}−*lp*-X (the latter being the distance between Pb^{II} and a ligand in the direction of the lone pair, opposite to the Pb^{II}−X direction) have been

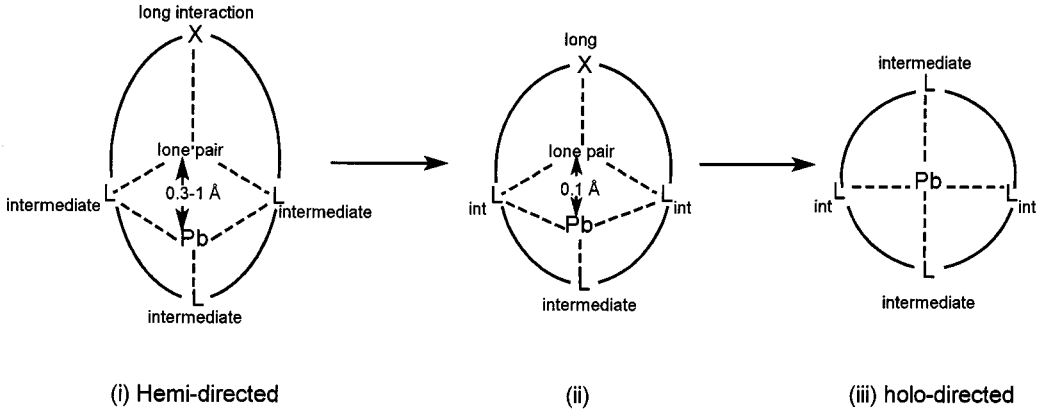

Figure 4. Hemi- and holo-direction

found to range from 0.3−1.2 Å. When the difference between these distances is small (ca. 0.1 Å), the coordination is regarded as holo-directed and the role of the lone pair becomes less clear, i.e. as to whether it exerts an effect on the stereochemistry (Figure 4). Generally speaking, hemi-directed ligand distribution is found for lead(II) compounds having coordination numbers 2−5, although lead(II) compounds having coordination numbers 6−8 have also been found to exhibit hemi-direction, particularly when harder oxygen and/or nitrogen donor atoms are available, as in the present set of ligands.[8]

Two important features of the structure of complex **1** are the empty zone in the coordination sphere about the lead(II) ion and the shortened distance between the metal and O(3) [Pb−O(3) 2.568(5) Å] relative to the other $Pb-O_{ether}$ distances. It is possible that these features may be directly attributed to a hemi-directed structure and the presence of a stereochemically active lone pair of electrons. However, this presumes that the perchlorate oxygen atoms O(3A) and O(4A) and the pendant amino nitrogen atom N(3) are distant from the lead [Pb−O(3A) 2.877, Pb−O(4A) 3.236, Pb−N(3) 2.892 Å] and thus not involved in coordination. If, however, the Pb−O(3A) and Pb−N(3) distances are considered as being long, ca. 0.3 Å in excess of the Pb−O(3) distance opposite, then the structure is close to the limit of being hemi-directed and the role of the lone pair is less clear.

Both aniline pendant arms are orientated on the same side of the macrocycle plane, resulting in a *syn* conformation, in contrast to the *anti* conformation found for free L^1. Planes containing the aromatic rings form an angle of 112.1°. Inspection of the crystal packing of **1** reveals that one of the two perchlorate anions is well-removed from the complex cation and has no interactions with neighbouring molecules. The second perchlorate anion, however, is involved in both a weak hydrogen-bonding interaction with a hydrogen atom on the non-coordinated pendant amino nitrogen atom N(3) [O(1A)···HN(3) 2.278 Å, O(1A)···N(3) 3.122 Å, O(1A)···HN(3)···N(3) 167.3°] and a weak interaction with the lead(II) atom [O(3A)···Pb 2.877 Å] (Figure 2b). This anion acts as a bridge between the metal and non-coordinated pendant amine group, thereby reinforcing the *syn* conformation present in complex **1**.

Synthesis and Characterization of Complexes of the Schiff-Base Lateral Macrobicycle L^3

Reaction of equimolar amounts of 2,6-diformylpyridine and *N*,*N*′-bis(2-aminobenzyl)-1,10-diaza-15-crown-5 (L^1) in the presence of lead(II) perchlorate in absolute ethanol under the conditions described in the Experimental Section gave the analytically pure product $[PbL^3](ClO_4)_2 \cdot EtOH$ (**3**) in 70% yield. The IR and FAB-mass spectra confirmed that condensation and [1+1] cyclization had occurred. Thus, the IR spectrum (KBr discs) of **3** features bands attributable to $\nu(C{=}N)_{imine}$ and $\nu(C{=}N)_{py}$ stretching modes at 1631 and 1583 cm^{-1}, respectively, but no bands due to carbonyl or amine vibration modes. The FAB-mass spectrum, obtained using 3-nitrobenzyl alcohol as the matrix, displays peaks at *m*/*z* (%) = 834 (37), 735 (20), and 528 (64) due to $[\mathbf{3} - (ClO_4)]^+$, $[\mathbf{3} - 2(ClO_4)]^+$, and $[L^3 + 1]^+$, respectively. Compound **3** can also be prepared by a transmetallation reaction using $[BaL^3](ClO_4)_2$ and lead(II) perchlorate; reaction in a 1:1 molar ratio in absolute ethanol solution gave **3** in 57% yield. The absence of peaks corresponding to species containing the BaL^3 fragment in the FAB-mass spectrum coupled with the presence of peaks due to $[\mathbf{3} - (ClO_4)]^+$, $[\mathbf{3} - 2(ClO_4)]^+$, and $[L^3 + 1]^+$ confirms that the transmetallation reaction has occurred and that the macrobicycle L^3 remains intact in the lead(II) complex.

^1H- and ^{13}C-NMR spectra recorded in acetonitrile solution also confirmed the integrity of the macrobicycle L^3 in this solvent; no resonances attributable to amino or aldehydic functions were seen. As expected, the signals due to the ethylenic protons of the crown moiety appear at high field as complicated multiplets as a result of the coordination of the metal by the oxygen atoms of the crown. The signals due to aromatic and pyridine protons, appearing at low field, are well-resolved and could be fully assigned. Considering the X-ray crystal structure (vide infra), two discrete signals due to the azomethine protons would be expected in the ^1H-NMR spectrum if structural integrity were to be maintained in solution. In fact, the spectrum recorded at 298 K features only one signal at δ = 9.09 (2 H) due to both of these protons. The spectrum recorded at 235 K shows a broadening of this signal, indicating a fluxional behaviour of **3** in acetonitrile solution. A striking feature of

the ^{1}H-NMR spectrum of this compound at 298 K is the rare observation of satellites attributable to proton coupling to the naturally abundant $I = 1/2$ nuclei of the metal, reflecting kinetic inertness in the complex as well as a degree of covalency in the interaction with a nearby donor atom. In the present case, the signal at $\delta = 9.09$ due to the imine protons appears as a singlet flanked by the satellites due to proton coupling to ^{207}Pb; the $^3J(^{207}\text{Pb-H}_{\text{imine}})$ coupling constant has a value of just 2.93 Hz, which corresponds with the weak $\text{Pb}-\text{N}_{\text{imine}}$ interaction observed in the crystal structure. Coupling to $I = 1/2$ metal nuclei is an emerging feature of the ^{1}H-NMR spectra of complexes containing the pyridine-2,6-diimine unit;[10,12,13] the case presented here would appear to be the third report of ^{207}Pb-^{1}H coupling in compounds of this type.

Attempted reactions between 2,6-diformylpyridine and L^1 in the presence of cadmium perchlorate under various experimental conditions yielded neither the expected cadmium complex of the Schiff-base macrobicycle L^3 nor uncoordinated L^3. In all cases, the IR spectra of the products exhibited bands attributable to $\nu(\text{C}=\text{N})_{\text{imine}}$ along with bands due to carbonyl and/or amine groups, thus indicating the presence of acyclic compounds. In contrast, a transmetallation reaction between $[\text{BaL}^3](\text{ClO}_4)_2$ and cadmium perchlorate in a 1:1 molar ratio gave rise to a yellow analytically pure product $[\text{CdL}^3](\text{ClO}_4)_2$ (**4**) in 55% yield. The FAB-mass spectrum, which features peaks due to $[\mathbf{4} - (\text{ClO}_4)]^+$, $[\mathbf{4} - 2\,(\text{ClO}_4)]^+$, and $[\text{L}^3 + 1]^+$ at *m/z* (%) = 740 (23), 641 (12), and 528 (100), respectively, and no peaks corresponding to species containing the BaL^3 fragment, provided initial evidence that the transmetallation reaction had indeed occurred and that the macrobicycle L^3 had remained intact in **4**. The IR spectrum features bands due to the C=N stretching modes of the imine and pyridine at 1641 and 1589 cm^{-1}, respectively, and bands due to the asymmetric stretching and bending modes of the perchlorate groups at 1095 and 623 cm^{-1}, respectively.

Conductivity measurements on 10^{-3} M solutions of the two cryptates in acetonitrile at 20 °C led to values of Λ_M = 291 cm$^2\Omega^{-1}$mol^{-1} for **3** and 266 cm$^2\Omega^{-1}$mol^{-1} for **4**, showing that both behave as 2:1 electrolytes in this solvent.[6] In the light of the X-ray crystal structure of **3** (vide infra), it is clear that its solution and solid-state structures must be different, the coordinated perchlorate anion being replaced by acetonitrile in solution.

X-ray Crystal Structure of 3

The crystal structure of the cryptate complex **3** contains the cation $[\text{PbL}^3(\text{ClO}_4)]^+$, a well-separated perchlorate anion, and a molecule of acetonitrile. Figure 5 shows a view of the structure of the cationic complex, while selected bond lengths and angles are given in Table 3. The metal ion is asymmetrically positioned in relation to the ligand cavity and only six of the eight available heteroatoms of L^3 are coordinated to it. One pivotal nitrogen atom and one imine nitrogen atom remain only weakly coordinated with long interactions [Pb−N(1) 2.857 Å, Pb−N(3) 2.837 Å]. This may possibly be linked to the influence of the lone pair as

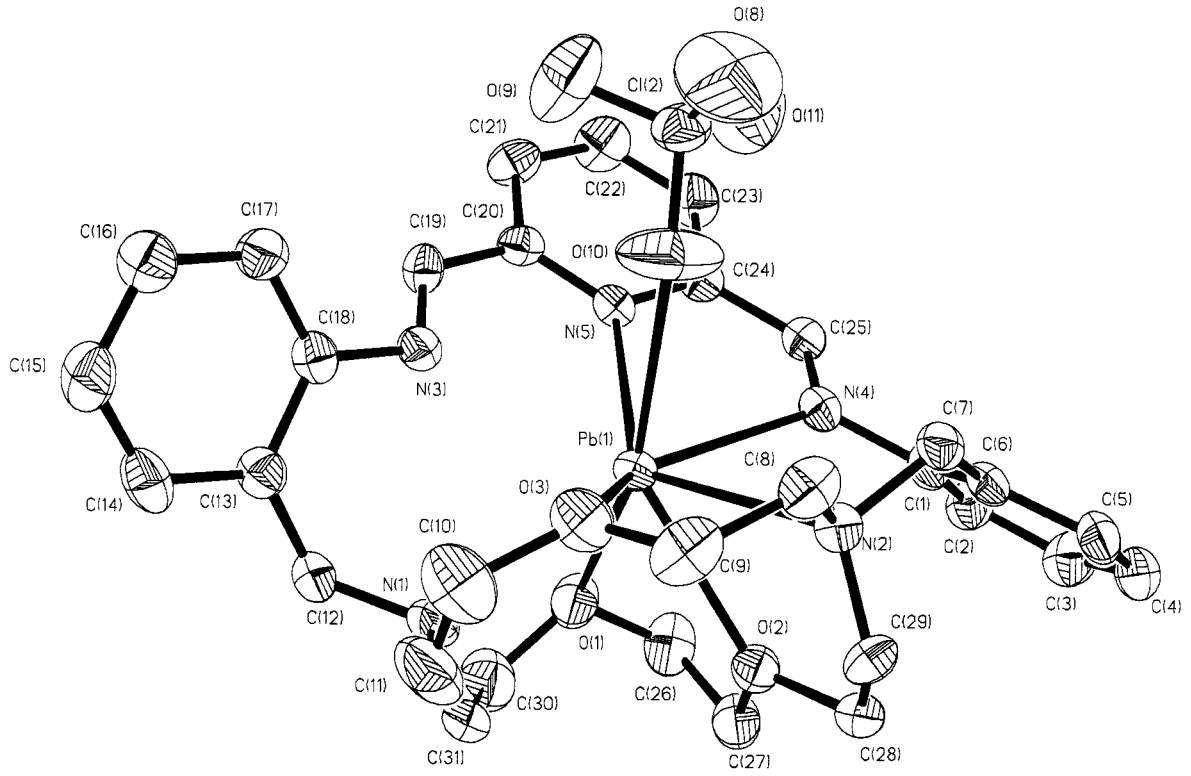

Figure 5. X-ray crystal structure of the cation of **3** with atom labelling; hydrogen atoms are omitted for simplicity; the ORTEP plot is drawn at a 30% probability level

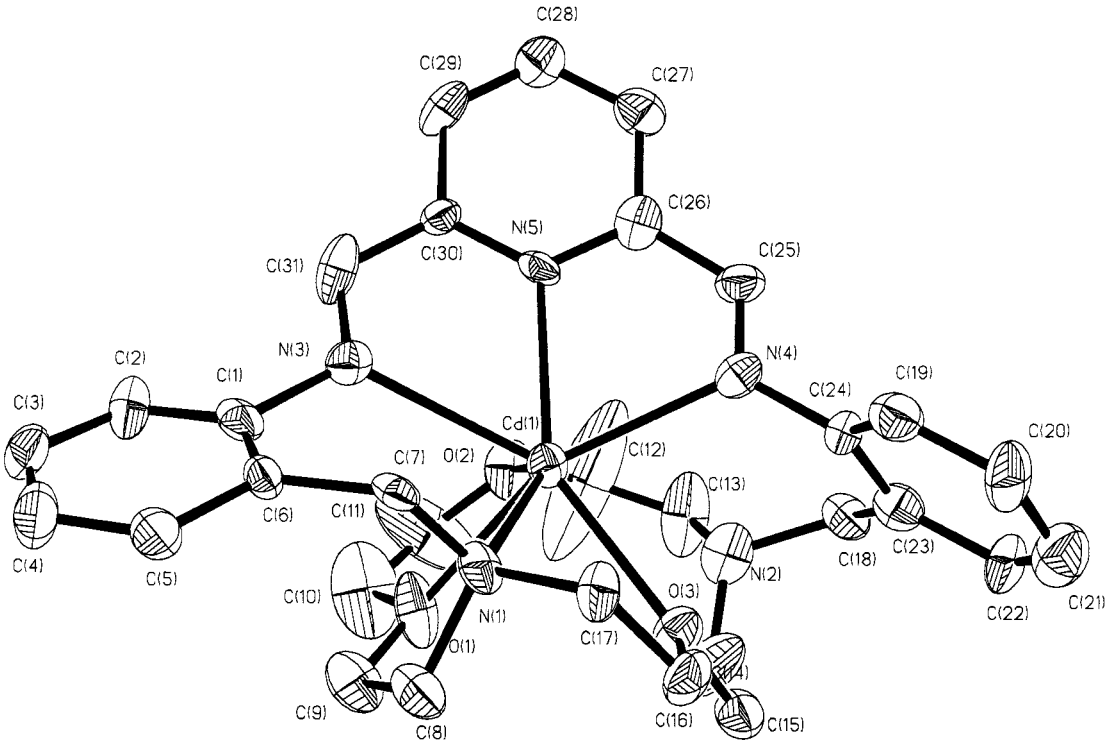

Figure 6. X-ray crystal structure of the cation of **4** with atom labelling; hydrogen atoms are omitted for simplicity; the ORTEP plot is drawn at a 30% probability level

discussed earlier. Two of the metal−oxygen bond lengths are practically equal [Pb−O(1) 2.718(6) Å, Pb−O(2) 2.719(6) Å] and slightly longer than the third [Pb−O(3) 2.670(6) Å]. These three distances fall within the range found for lead(II) crown-ether complexes;[7] the first is shorter than the corresponding distance found in compound **2**, whereas the other two are slightly longer. The distance of 2.740(6) Å for Pb−N(4) is also within the usual range found for lead(II) imine complexes,[12,14] while the Pb−N(5) distance is slightly longer than typically observed $Pb-N_{pyridine}$ distances.[15] The coordination sphere of the lead is completed by one oxygen atom of a monodentate perchlorate group and the coordination polyhedron may be described as a dodecahedron with an unoccupied site. The lateral aromatic rings of the cryptand L^3 are in different planes, which intersect at 87.2°. The pyridine ring and the two imine groups are coplanar and their plane forms dihedral angles of 52.9° with the plane containing the benzene ring bound to N(1) and 49.7° with the plane containing the other aromatic ring.

X-ray Crystal Structure of 4

Figure 6 shows the structure of the dication $[CdL^3]^{2+}$ in crystals of $[CdL^3](ClO_4)_2$ (**4**). Selected bond distances and angles are given in Table 3. The cadmium(II) ion resides in a distorted monocapped octahedral N_4O_3 environment, bound by seven of the eight donor atoms of the macrobicyclic receptor; the pivotal nitrogen N(2) is rather distant from the metal ion [Cd−N(2) 3.134 Å] and remains uncoordinated. The bond lengths between the imine nitrogen atoms and the cadmium ion differ by 0.147 Å and fall within the range reported for similar bonds in X-ray crystal structures containing similar fragments.[14,16] The cadmium is positioned slightly closer to O(1) (2.374 Å) than to the other two oxygen atoms (2.493, 2.459 Å). As in the lead(II) cryptate **3**, the pyridine ring and the two imine groups are coplanar although in **4** this plane forms dihedral angles of 145.7° with the plane containing the benzene ring bound to N(1) and 96.9° with plane of the other aromatic ring; the lateral aromatic rings of L^3 are in different planes which intersect at 61°.

Discussion

Two points of interest emerge from the above data. The first relates to the synthetic strategies followed in preparing the lead(II) and cadmium(II) cryptates with the Schiff-base lateral macrobicycle L^3 (compounds **3** and **4**), while the second concerns the different complexation capabilities of the two types of macrocycles (lariat ether L^1 and macrobicycle L^3) towards the heavy metal ions lead(II) and cadmium(II), as well as the influence of the nature of the metal ion guest on the conformation adopted by the macrobicycle receptor L^3.

In a previous paper,[4] we reported that it proved impossible to prepare the Schiff-base lateral macrobicycle L^3 by a direct reaction between the organic precursors due to the *anti* arrangement adopted by the diamine L^1, not only in the solid state but also in solution, and that a barium cation

was required to template the reaction between L^1 and 2,6-diformylpyridine to build L^3. Herein, we have shown that the corresponding lead(II) and cadmium(II) cryptates of L^3 can be prepared by transmetallation reactions starting from the barium cryptate (Scheme 2). This indicates a coordinative preference of L^3 for these soft metal ions.

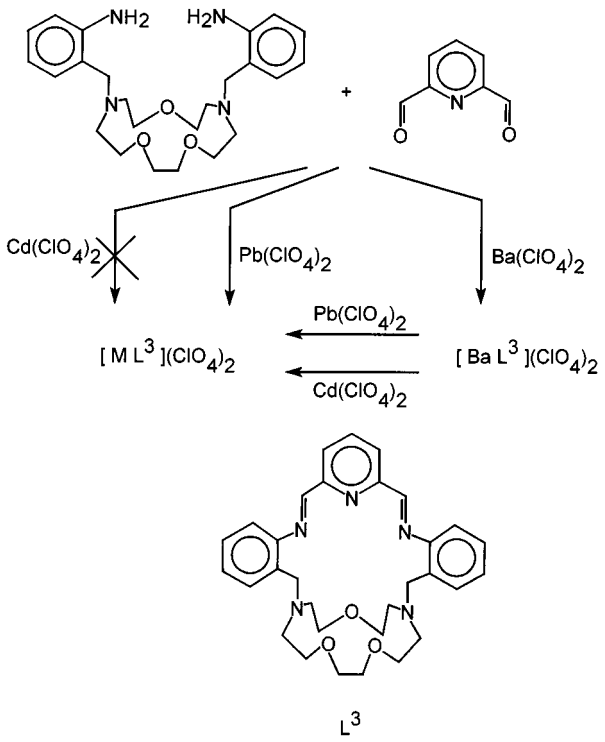

Scheme 2

The efficiencies of these soft metal ions as template agents in the synthesis of L^3 have been studied. Whereas the lead(II) ion was found to be capable of acting as an effective template in this synthesis, this was not the case with the cadmium ion. The effectiveness of lead in the templating process stems from its ability to orientate the pendant arms of the diamine L^1 in a *syn* conformation. This is evident in the X-ray crystal structure of the lead(II) complex of L^1 (**1**) and the situation is likely to be maintained in solution. An important feature of the structure of **1** is the *syn* conformation of the bibracchial macrocyclic ligand L^1, even when one pendant arm is not directly coordinated to the metal. A *syn* arrangement of L^1 has also been observed in the crystal structure of the barium complex $[BaL^1](ClO_4)_2$,[4] while an *anti* arrangement has been found in the crystal structure of the octahedral copper(II) complex $[CuL^1](ClO_4)_2$.[17] It seems likely that the disposition of the pendant arms in complexes of L^1 is related to the size of the cation present. The copper(II) cation (r_{CN4} = 0.57; r_{CN6} = 0.73 Å),[18] with a penchant for square-planar geometry, resides in the macrocyclic cavity bound by two ether oxygen and two pivotal amino nitrogen atoms. The donor atoms of the pendant arms coordinate apically so as to form an octahedral coordination sphere. The larger barium cation (r_{CN9} = 1.47 Å)[18] may be regarded as spherically symmetrical and the geometries found in its complexes are not constrained by *d*-orbital orthogonality or crystal-field stabilization energies. Consequently, in $[BaL^1](ClO_4)_2$ the barium is found in a position that allows optimal interaction with the seven ligand donor atoms and a bidentate perchlorate anion. This necessitates a *syn* orientation of the pendant arms and the overall structure resembles that of molecular clefts reported for barium complexes of bibracchial tetraimine Schiff-base macrocycles,[19–21] and for potassium and barium complexes of the related lariat ethers derived from the larger [18-aneN_2O_4] macrocyclic polyether with alcohol-bearing 2-hydroxy-1,1-dimethylethyl and [(2-hydroxyethyl)oxy]ethyl pendant arms.[22,23] The lead(II) cation is intermediate in size (r_{CN6} = 1.19 Å)[18] and its geometry is free of *d*-orbital control, as a result of which it resides above the macrocyclic cavity towards the pendant arms, one of which coordinates weakly [Pb–N(3) 2.892 Å]. It can also be suggested that the ineffectiveness of the cadmium ion as a template agent in the synthesis of the macrobicycle L^3 stems from the unsuitable conformation adopted by the diamine L^1 in the presence of this metal ion. Considering the small size of the cadmium ion (r_{CN6} = 0.95 Å) and in the light of spectroscopic characterization of the cadmium complex of the diamine L^1 (**2**), it can be stated that the metal ion lies inside the cavity of the crown in a coordination environment rather similar to that found for the copper complex;[17] L^1 must therefore adopt an *anti* arrangement.

Viewing the crystal structures of cryptates **3** and **4**, as well as that of the corresponding barium cryptate,[4] from a side perspective through the axis of the pivotal nitrogen atoms (Figure 7) allows an appraisal of the influence of the metal ion on the conformation of the macrobicycle receptor L^3. The most significant changes concern the folding of the crown, the distance between the two pivotal nitrogen atoms, and the distance between the imine nitrogen atoms. In the case of the barium cryptate (Figure 7a), the crown moiety folds in such a way that both pivotal nitrogen atoms and the two oxygen atoms of one chain form a plane (deviation from planarity 0.0425 Å). However, in neither the lead cryptate **3** nor the cadmium cryptate **4** is it possible to find a plane formed by four of the six donor atoms of the crown moiety of L^3. While the distance between the two pivotal nitrogen atoms [N(1)–N(2)] is clearly longer in the case of **4** (4.870 Å) than in the case of **3** (4.688 Å), the distance between the imine nitrogen atoms [N(3)–N(4)] is shorter in the case of **4** (4.442 Å) than in the case of **3** (4.855 Å). In both cryptates, these distances are considerably shorter than the corresponding distances in the barium cryptate, which amount to 5.389 Å and 5.002 Å, respectively. These data illustrate how the macrobicycle L^3 can either expand or contract in order to accommodate the metal ion in its cavity, in spite of the presence of a relatively rigid unsaturated chelating chain in its backbone. Some minor differences are evident from the values of the angles N(pivotal)–C–C(aryl); whereas angles N(1)–C(7)–C(6) and N(2)–C(18)–C(23) in complex **4** are practically equal, having values of 115.8(10)° and 115.3(11)°, respectively, the

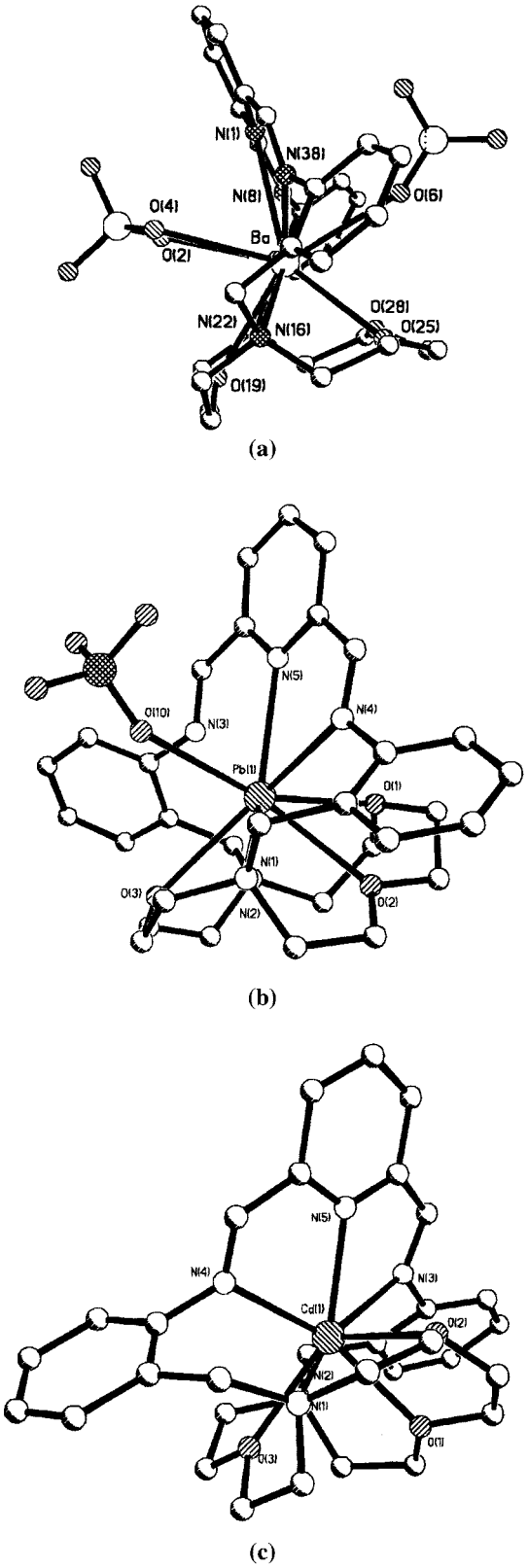

Figure 7. Side view of (a) $[BaL^3]^{2+}$(see ref.[4]), (b) $[PbL^3(ClO_4)]^+$, and (c) $[CdL^3]^{2+}$

corresponding angles in **3** have values of 114.7(7)° and 117.0(8)°.

The effect of the pyridine moiety on the arrangement of the diamine fragment in the case of lead(II) cryptate **3** can be also appreciated by comparing the X-ray crystal structure of this complex with that of the lead(II) complex with the bibracchial lariat ether L^1 (**1**). The folding of the crown moiety is clearly different in the two compounds. In **1**, the three oxygen atoms and the pivotal nitrogen N(2) form a plane (deviation from planarity 0.077 Å), with the lead(II) ion residing 1.652 Å above it, in contrast to the situation in **3**. Moreover, the distance between the two pivotal nitrogen atoms [N(1)−N(2)] is clearly longer in **1** (4.881 Å) than in **3** (4.688 Å).

Concluding Remarks

The Schiff-base lateral macrobicycle L^3 has been shown to act as a receptor for both lead(II) and cadmium(II) guests. The respective cryptates can be prepared by simple transmetallation reactions starting from the analogous barium cryptate, which highlights the preference of L^3 for the heavy metal ions. The lead(II) ion has been found to be capable of acting as a template agent in the synthesis of L^3, whereas this is not the case for the cadmium(II) ion.

The nature of the guest metal ion has been found to have a significant influence on the conformation adopted by the receptor L^3. Macrobicycle L^3 can either expand or contract to accommodate the metal ion in its cavity, in spite of the fact that its backbone incorporates a relatively rigid unsaturated chelating chain.

Experimental Section

Measurements: Elemental analyses and FAB-MS spectra were provided by the Servicios Xerais de Apoio á Investigación of the Universidade da Coruña; elemental analyses were carried out on a Carlo Erba 1180 elemental analyzer, and FAB-MS spectra were recorded on a Fisons Quatro mass spectrometer with a Cs^+ ion gun using 3-nitrobenzyl alcohol as a matrix. − ^{1}H- and ^{13}C-NMR spectra were recorded on a Bruker AC 200 F or a Bruker WM-500 spectrometer. − IR spectra were recorded from samples between KBr discs on a Perkin−Elmer 1330 spectrophotometer. − UV/vis spectra were recorded on a Uvikon 942 Plus spectrophotometer. − Melting points were measured on a Gallenkamp apparatus. − Conductivity measurements were carried out at 20 °C with a Crison Micro CM 2201 conductivimeter using 10^{-3} M solutions of the complexes in acetonitrile.

Materials: 2,6-Diformylpyridine was synthesized according to literature methods.[24,25] The barium cryptate $[BaL^3](ClO_4)_2$ was prepared as described previously.[4] All other chemicals were purchased from commercial sources and used without further purification. Solvents were of reagent grade and were purified by the usual methods.

Caution! Although we have experienced no difficulties with the perchlorate salts, these should be regarded as potentially explosive and handled with care.

Preparation of *N*,*N*′-Bis(2-aminobenzyl)-1,10-diaza-15-crown-5 (L^1): A solution of 2-nitrobenzyl chloride (1.6 g, 9.2 mmol) in acetonitrile (20 mL) was added to a stirred solution of 1,10-diaza-15-

crown-5 (1.0 g, 4.6 mmol) and Na_2CO_3 (2.4 g, 23 mmol) in acetonitrile (30 mL). The reaction mixture was stirred under reflux for 24 h. It was then filtered, the filtrate was concentrated, and the yellow oily residue was extracted with CH_2Cl_2/water. The organic phase was dried with anhydrous $MgSO_4$ and concentrated in vacuo. The resulting yellow oil was dissolved in absolute ethanol (60 mL) and Pd/C was added. Hydrazine hydrate (1.5 mL) was slowly added and the reaction mixture was heated and stirred for 24 h. It was then filtered and the solvent was removed from the filtrate in a rotary evaporator. Addition of cold diethyl ether to the oily residue led to the deposition of a white precipitate. Recrystallization from absolute ethanol/diethyl ether (1:1) gave crystals suitable for X-ray diffraction analysis. Yield: 1.2 g (61%); m.p. 92−94 °C. − $C_{24}H_{36}N_4O_3$: calcd. C 67.2, H 8.5, N 13.1; found C 66.7, H 8.5, N 13.1. − ^{13}C NMR (500 Mz, CD_3CN): δ = 54.1, 54.2 (C-3, C-1), 59.1 (C-6), 69.2, 68.3 (C-5, C-2), 70.0 (C-4), 114.9 (C-11), 116.4 (C-9), 122.9 (C-7), 128.0 (C-10), 130.1 (C-8), 148.1 (C-12). − FAB-MS: *m/z* = 429 [L^1 + 1]. − IR (KBr discs): ṽ = 3430, 3390, 3293, 3275 (NH_2), 1618, 1495, 1463, 1448 (C=C) cm^{-1}.

Preparation of the Complexes

[PbL^1](ClO$_4$)$_2$ (1): A solution of $Pb(ClO_4)_2 \cdot H_2O$ (0.11 g, 0.26 mmol) in absolute ethanol (5 mL) was added to a stirred solution of the ligand L^1 (0.12 g, 0.26 mmol) in absolute ethanol (10 mL). The reaction mixture was stirred under reflux for 6 h. During the course of the reaction, the solution became turbid and a white precipitate was deposited. This was collected by filtration, washed with absolute ethanol, and dried in air. Slow diffusion of diethyl ether into a solution of **1** in acetonitrile gave crystals suitable for X-ray crystallography. Yield: 0.15 g (73%); m.p. 268 °C (decomp.). − $C_{24}H_{36}Cl_2N_4O_{11}Pb$: calcd. C 34.5, H 4.3, N 6.7; found C 34.6, H 4.3, N 6.7. − ^{13}C NMR (200 Mz, CD_3CN): δ = 53.1, 53.2 (C-3, C-1), 56.5 (C-6), 70.0, 69.5, 68.4 (C-5, C-4, C-2), 121.4 (C-11), 123.7 (C-9), 125.1 (C-7), 131.5 (C-10), 134.6 (C-8), 142.5 (C-12). − FAB-MS: *m/z* = 735 [**1** − ClO_4], 635 [**1** − 2 ClO_4]. − IR (KBr discs): ṽ = 3334, 3277 (NH_2), 1613, 1586, 1495, 1457 (C=C), 1110, 617 (ClO_4) cm^{-1}.

[CdL^1](ClO$_4$)$_2$ (2): This white complex was prepared as described for **1** by using $Cd(ClO_4)_2$ (0.10 g, 0.26 mmol). Yield: 0.13 g (65%); m.p. 308 °C (decomp.). − $C_{24}H_{36}CdCl_2N_4O_{11}$: calcd. C 38.9, H 4.9, N 7.6; found C 39.1, H 4.6, N 7.5. − FAB-MS: *m/z* = 641 [**2** − ClO_4], 541 [**2** − 2 ClO_4]. − IR (KBr discs): ṽ = 3320, 3281 (NH_2), 1617, 1590, 1499, 1464 (C=C), 1110, 623 (ClO_4) cm^{-1}.

[PbL^3](ClO$_4$)$_2$·EtOH (3) − Method A: A solution of $Pb(ClO_4)_2 \cdot H_2O$ (0.048 g, 0.100 mmol) in absolute ethanol (5 mL) was added to a stirred solution of [BaL^3](ClO$_4$)$_2$ (0.045 g, 0.050 mmol) in absolute ethanol (35 mL) and the resulting mixture was stirred under reflux for one day. During the course of the reaction, the solution became deep-yellow. It was filtered while still hot, and then the filtrate was allowed to cool to room temperature. A yellow microcrystalline precipitate formed, which was collected by filtration. Yield: 0.039 g (57%); m.p. 333 °C (decomp.). − $C_{31}H_{37}Cl_2N_5O_{11}Pb \cdot EtOH$: calcd. C 40.45, H 4.4, N 7.1; found C 40.5, H 4.5, N 7.0.

Method B: A solution of $Pb(ClO_4)_2 \cdot H_2O$ (0.122 g, 0.25 mmol) in absolute ethanol (50 mL) was added to a stirred solution of *N*,*N*′-bis(2-aminobenzyl)-1,10-diaza-15-crown-5 (0.114 g, 0.250 mmol) in absolute ethanol (120 mL). The mixture was vigorously stirred and heated while a solution of 2,6-diformylpyridine (0.036 g, 0.250 mmol) in absolute ethanol (60 mL) was added dropwise during the course of a day. After the addition was complete, the resulting pale-yellow solution was stirred under reflux for a further day. The solution was filtered while hot; upon cooling the filtrate to room temperature, a pale-yellow microcrystalline precipitate formed, which was collected by filtration. Yield: 0.170 g (70%). − $C_{31}H_{37}Cl_2N_5O_{11}Pb \cdot EtOH$: calcd. C 40.45, H 4.4, N 7.1; found C 40.7, H 4.4, N 6.9. − ^{13}C NMR (200 Mz, CD_3CN): δ = 57.8, 58.2, 58.8, 69.1, 69.6, 121.2, 129.4, 131.3, 131.8, 132.6, 133.5, 142.6, 150.1, 154.2, 164.6. − FAB-MS: *m/z* = 834 [**3** − ClO_4], 735 [**3** − 2 ClO_4]. − IR (KBr discs): ṽ = 1631 $(C=N)_{imine}$, 1583 $(C=N)_{py}$, 1490, 1456 (C=C), 1093, 623 (ClO_4) cm^{-1}. Slow diffusion of diethyl ether into a solution of **3** in acetonitrile gave crystals suitable for X-ray crystallography.

[CdL^3](ClO$_4$)$_2$ (4): A solution of $Cd(ClO_4)_2$ (0.038 g, 0.100 mmol) in absolute ethanol (5 mL) was added to a stirred solution of [BaL^3-$(ClO_4)_2$] (0.045 g, 0.050 mmol) in absolute ethanol (35 mL) and the resulting mixture was stirred under reflux for one day. During the course of the reaction, the solution became turbid and a yellow precipitate was deposited. This was collected by filtration, washed

Table 4. Crystallographic details for L^1, **1**, **3**, and **4**

	L^1	**1**	**3**	**4**
Empirical formula	$C_{24}H_{36}N_4O_3$	$C_{24}H_{36}Cl_2N_4O_{11}Pb$	$C_{33}H_{39}Cl_2N_6O_{11}Pb$	$C_{31}H_{39}Cl_2N_5O_{12}Cd$
Form. wt.	428.57	834.66	873.79	856.97
Space group	$P\bar{1}$	$P\bar{1}$	$P2(1)/c$	$P\bar{1}$
Crystal system	Triclinic	Triclinic	Monoclinic	Triclinic
Z	2	2	4	2
a [Å]	10.249(2)	8.8027(5)	17.333(5)	10.4634(9)
b [Å]	10.405(4)	10.7781(6)	13.314(4)	10.5331(8)
c [Å]	12.157(3)	16.4298(8)	16.375(6)	17.6224(14)
α [°]	86.97(4)	91.1770(10)	90	95.204(2)
β [°]	70.050(10)	105.2300(10)	93.94(2)	100.293(2)
γ [°]	78.58(3)	100.5180(10)	90	113.716(2)
V [Å^3]	1194.4(6)	1474.92(14)	3770.0(21)	1720.8(2)
$\rho_{calcd.}$ [g/cm^3]	1.192	1.879	1.716	1.654
$\mu_{calcd.}$ [mm^{-1}]	0.079	5.965	4.683	0.861
Radn. (Mo-K_α) [Å]	0.71073	0.71073	0.71073	0.71073
T [K]	293(2)	298(2)	293(2)	298(2)
Final *R* indices[a]	R_1 = 0.0660	R_1 = 0.0440	R_1 = 0.0474	R_1 = 0.0845
[$I > 2\sigma(I)$]	wR_2 = 0.1755	wR_2 =0.1025	wR_2 = 0.0971	wR_2 = 0.1883
Final *R* indices	R_1 = 0.0845	R_1 = 0.0524	R_1 = 0.0830	R_1 = 0.1862
(for all data)	wR_2 = 0.1930	wR_2 = 0.111	wR_2 = 0.1119	wR_2 = 0.2501

[a] $R_1 = \Sigma||F_o|-|F_c||/\Sigma|F_o|$ and $wR_2 = \{\Sigma[w(|F_o|^2-|F_c|^2|)^2]/\Sigma[w(F_o^4)]\}^{1/2}$.

with absolute ethanol, and dried in air. X-ray quality crystals were grown by slow diffusion of diethyl ether into a solution of **4** in acetonitrile. Yield: 0.033 g (55%); m.p. 280 °C (decomp.). − $C_{31}H_{37}CdCl_2N_5O_{11}$: calcd. C 43.9, H 4.5, N 8.2; found C 43.8, H 4.1, N 8.3. − FAB-MS: *m/z* = 740 [**4** − ClO_4], 641 [**4** − 2 ClO_4]. − IR (KBr discs): $\tilde{\nu}$ = 1641 $(C{=}N)_{imine}$, 1589 $(C{=}N)_{py}$, 1487, 1461, 1449 (C=C), 1095, 623 (ClO_4) cm^{-1}.

X-ray Crystallographic Study − Crystal Structure Determinations of L^1 and Complex 3: Macrocycle $\mathbf{L^1}$ was crystallized from absolute ethanol/diethyl ether (1:1) in the form of colourless blocks (dimensions of the selected crystal: 0.85 × 0.43 × 0.25 mm^3). Complex **3** was crystallized in the form of yellow blocks by slow diffusion of diethyl ether into an acetonitrile solution (dimensions of the selected crystal: 0.76 × 0.45 × 0.32 mm^3). X-ray data were collected at room temperature in the range $3.5 < 2\varphi < 50°$ on a Siemens P4 diffractometer by the ω-scan method. 4972 reflections were measured for L^1, 8062 for **3**, all of which were corrected for Lorentz and polarization effects and for absorption by the analysis of 10 azimuthal scans (minimum and maximum transmission coefficients 0.4373 and 0.9788 for L^1, 0.273 and 0.709 for **3**); 3218 and 4656 independent reflections, respectively, exceeded the significance level $F/\sigma(F) > 4.0$. The structure was solved by direct methods and refined by full-matrix least-squares methods on F^2. Hydrogen atoms were included in calculated positions and refined in riding mode. For L^1, convergence was reached at a final R = 0.0660, wR_2 = 0.1930; 281 parameters for all 4201 unique data, allowing for the thermal anisotropy of all non-hydrogen atoms. Minimum and maximum final electron density: −0.396 and 0.859 $eÅ^{-3}$. For **3**, convergence was reached at a final R = 0.0474, wR_2 = 0.0971; 468 parameters for all 6631 unique data, allowing for the thermal anisotropy of all non-hydrogen atoms. No residual density was found outside −0.613 and 0.648 $eÅ^{-3}$. In all cases, complex scattering factors were taken from the program package SHELXL-93[26] as implemented on a Viglen 486dx computer. Crystal data and details of the data collection and refinement are presented in Table 4.

Crystal Structure Determinations of Complexes 1 and 4: Both were crystallized in the form of yellow blocks by slow diffusion of diethyl ether into acetonitrile solutions (dimensions of the selected crystals: 0.55 × 0.25 × 0.15 mm^3 for **1** and 0.35 × 0.15 × 0.10 mm^3 for **4**). X-ray data for **1** and **4** were collected on a Siemens SMART CCD area detector single-crystal diffractometer operating at room temperature. Preliminary unit cell constants were determined from a set of 45 narrow-frame (0.3° in ω) scans. A total of 1255 frames of intensity data were collected with a frame width of 0.3° each in ω and a counting time of 10 s/frame at a crystal-to-detector distance of 4.0 cm. The collected frames were integrated using an orientation matrix determined from the narrow-frame scans and refined using Siemens SAINT software on all the observed reflections. A semiempirical absorption correction using an ellipsoidal model (maximum and minimum transmission coefficients 0.455 and 0.299) was applied for **1**, whereas an absorption correction using the SADABS program (maximum and minimum transmission coefficients 1.000 and 0.467) was applied for **4**. The integration process yielded 8176 reflections, of which 5118 were independent for **1**, and 8855 reflections, of which 5693 were independent for **4**. The structures were solved by Patterson and Fourier methods using Siemens SHELXTL-PC software[27] and refined by full-matrix least-squares methods on F^2. Hydrogen atoms were included in calculated positions and refined in riding mode. For **1**, convergence was reached at R = 0.0440, wR_2 = 0.1026; 379 parameters for all 5056 unique data, allowing for the thermal anisotropy of all non-hydrogen atoms. A final difference Fourier map showed no residual density outside −1.624 and 1.574 $eÅ^{-3}$. For **4**, convergence was reached at R = 0.0883, wR_2 = 0.1972; 460 parameters for all 5693 unique data, allowing for the thermal anisotropy of all non-hydrogen atoms; minimum and maximum final electron density: −0.829 and 1.431 $eÅ^{-3}$. Crystal data and details of the data collection and refinement are summarized in Table 4.

Crystallographic data (excluding structure factors) for the structures reported in this paper have been deposited with the Cambridge Crystallographic Data Centre as supplementary publication nos. CCDC-136178, CCDC-136179, CCDC-136180, and CCDC-136181. Copies of the data can be obtained free of charge on application to the CCDC, 12 Union Road, Cambridge CB2 1EZ, U.K. [Fax: (internat.) +44 (0)1223/336033; E-mail: deposit@ccdc.cam.ac.uk].

Acknowledgments

The authors thank the Universidade da Coruña for financial support.

[1] [1a] F. Vögtle, E. Weber (Eds.), *Host-Guest Complex Chemistry: Macrocycles*, Springer, Berlin, Heidelberg, **1985**. − [1b] R. M. Izatt, J. J. Christensen (Eds.), *Synthesis of Selective Agents (Progress in Macrocyclic Chemistry)*, Wiley, New York, **1987**, vol. 3. − [1c] J.-M. Lehn, F. Montavon, *Helv. Chim. Acta* **1978**, *61*, 67.

[2] [2a] Y. Inoue, G. W. Gokel (Eds.), *Cation Binding by Macrocycles*, Marcel Dekker, New York, **1990**. − [2b] G. W. Gokel, *Crown Ethers and Cryptands*, The Royal Society of Chemistry, Cambridge, **1991**.

[3] A. T. Yordanov, D. M. Roundhill, *Coord. Chem. Rev.* **1998**, *170*, 93.

[4] D. Esteban, D. Bañobre, R. Bastida, A. de Blas, A. Macías, A. Rodríguez, T. Rodríguez-Blas, D. E. Fenton, H. Adams, J. Mahía, *Inorg. Chem.* **1999**, *38*, 1937.

[5] According to J.-M. Lehn, *Pure & Appl. Chem.* **1980**, *52*, 2441, *lateral macrobicycles* are dissymetrical molecules structurally based on the combination of two different binding subunits, a chelating one and a macrocyclic one.

[6] W. J. Geary, *Coord. Chem. Rev.* **1971**, *7*, 81.

[7] R. D. Rogers, A. H. Bond, *Inorg. Chim. Acta* **1992**, *192*, 163.

[8] L. Shimoni-Livny, J. P. Glusker, C. W. Bock, *Inorg. Chem.* **1998**, *37*, 1853.

[9] R. D. Hancock, M. S. Shaikjee, S. M. Dobson, J. C. A. Boeyens, *Inorg. Chim. Acta* **1988**, *154*, 229.

[10] A. Bashall, M. McPartlin, B. P. Murphy, H. R. Powell, S. Waikar, *J. Chem. Soc., Dalton Trans.* **1994**, 1383.

[11] R. D. Hancock, *Perspectives in Coordination Chemistry* (Eds.: A. F. Williams, C. Floriani, A. E. Merbach), Verlag HCA, Basel, **1992**, p. 129.

[12] D. E. Fenton, R. W. Mathews, M. McPartlin, B. P. Murphy, I. J. Scowen, P. A. Tasker, *J. Chem. Soc., Dalton Trans.* **1996**, 3421.

[13] [13a] M. G. B. Drew, D. Marrs, J. Hunter, J. Nelson, *J. Chem. Soc., Dalton Trans.* **1992**, 11. − [13b] P. S. Marchetti, S. Bank, T. W. Bell, M. A. Kennedy, P. D. Ellis, *J. Am. Chem. Soc.* **1989**, *111*, 2063. − [13c] M. G. B. Drew, D. McDowell, J. Nelson, *Polyhedron* **1988**, *7*, 2229.

[14] M. G. B. Drew, O. W. Howarth, G. G. Morgan, J. Nelson, *J. Chem. Soc., Dalton Trans.* **1994**, 3149.

[15] E. C. Constable, C. Sacht, G. Palo, D. A. Tocher, M. R. Truter, *J. Chem. Soc., Dalton Trans.* **1993**, 1307, and references therein.

[16] [16a] M. G. B. Drew, J. de O. Cabral, M. F. Cabral, F. S. Esho, S. M. Nelson, *J. Chem. Soc., Chem. Commun.* **1979**, 1033. − [16b] S. M. Nelson, S. G. McFall, M. G. B. Drew, A. H. B. Othman, B. Mason, *J. Chem. Soc., Chem. Commun.* **1977**, 167. − [16c] M. G. B. Drew, S. G. McFall, S. M. Nelson, *J. Chem. Soc., Dalton Trans.* **1979**, 575. − [16d] K. R. Adam, S. Donnelly, A. J. Leong, L. F. Lindoy, B. J. McCool, A. Bashall, M. R. Dent, B. P.

Murphy, M. McPartlin, D. E. Fenton, P. A. Tasker, *J. Chem. Soc., Dalton Trans.* **1990**, 1635.
[17] C. Rodriguez-Infante, D. Esteban, R. Bastida, A. De Blas, A. Macías, A. Rodríguez, T. Rodríguez-Blas, D. E. Fenton, J. Mahía, unpublished results.
[18] R. D. Shannon, *Acta Cryst.* **1976**, *A36*, 752.
[19] H. Adams, N. A. Bailey, W. D. Carlisle, D. E. Fenton, G. Rossi, *J. Chem. Soc., Dalton Trans.* **1990**, 1271.
[20] N. A. Bailey, A.Rodriguez, C. O. Barbarin, D. E. Fenton, P. C. Hellier, P. D. Hempstead, M. Kanesato, P. B. Leeson, *J. Chem. Soc., Dalton Trans.* **1995**, 765.
[21] H. Adams, N. A. Bailey, S. R. Collinson, D. E. Fenton, C. J. Harding, S. J. Kitchen, *Inorg. Chim. Acta* **1996**, *246*, 81.
[22] K. V. Damic, R. D. Hancock, P. W. Wade, J. C. A. Boeyens, D. G. Billing, S. M. Dobson, *J. Chem. Soc., Dalton Trans.* **1991**, 293.
[23] R. Bhavan, R. D. Hancock, P. W. Wade, J. C. A. Boeyens, S. M. Dobson, *Inorg. Chim. Acta* **1990**, *171*, 235.
[24] E. P. Papadoupoulus, A. Jarrar, C. H. Issidorides, *J. Org. Chem.* **1966**, *31*, 615.
[25] D. Jerchel, J. Heider, H. Wagner, *Liebigs Ann. Chem.* **1958**, *613*, 153.
[26] G. M. Sheldrick, *SHELXL-93*, *An integrated system for solving and refining crystal structures from diffraction data*, University of Göttingen, Germany, **1993**.
[27] G. M. Sheldrick, *SHELXTL-PC*, *An integrated system for solving and refining crystal structures from diffraction data*, University of Göttingen, Germany, **1997**.

Received October 25, 1999
[I99375]